ment of radiosensitivity by proteasome inhibition: implications for a role of NF-κB. *Int. J. Radiat. Oncol. Biol. Phys.*, **50**, 183–193 (2001).

30) Zhong, H., Voll, R. E., and Ghosh, S., Phosphorylation of NF-κB p65 by PKA stimulates transcriptional activity by promoting a novel bivalent interaction with the coactivator CBP/p300. *Mol. Cell*, **1**, 661–671 (1998).

31) Wang, D., Westerheide, S. D., Hanson, J. L., and Baldwin, A. S., Jr., Tumor necrosis factor-induced phosphorylation of RelA/p65 on ser529 is controlled by casein kinase II. *J. Biol. Chem.*, **275**, 32592–32597 (2000).

32) Feling, R. H., Buchanan, G. O., Mincer, T. J., Kauffman, C. A., Jensen, P. R., and Fenical, W., Salinosporamide A: a highly cytotoxic proteasome inhibitor from a novel microbial source, a marine bacterium of the new genus salinospora. *Angew. Chem.*, **42**, 355–357 (2003).

33) Chauhan, D., Catley, L., Li, G., Podar, K., Hideshima, T., Velankar, M., Mitsiades, C., Mitsiades, N., Yasui, H., Letai, A., Ovaa, H., Berkers, C., Nicholson, B., Chao, T. H., Neuteboom, S. T., Richardson, P., Palladino, M. A., and Anderson, K. C., A novel orally active proteasome inhibitor induces apoptosis in multiple myeloma cells with mechanisms distinct from Bortezomib. *Cancer Cell*, **8**, 407–419 (2005).

Jpn J Clin Oncol 2008;38(12)793–802
doi:10.1093/jjco/hyn116

Review Article

Polymeric Micellar Delivery Systems in Oncology

Yasuhiro Matsumura

Investigative Treatment Division, Research Center for Innovative Oncology, National Cancer Center Hospital East, Kashiwa, Chiba, Japan

Received September 1, 2008; accepted September 22, 2008; published online November 6, 2008

The purpose of drug delivery systems in cancer chemotherapy is to achieve selective delivery of anti-cancer agents to cancer tissue at an effective concentrations for the appropriate duration of time, so that we may be able to reduce the adverse effects of a drug and simultaneously enhance the anti-tumor effect. Polymeric micelles were expected to increase the accumulation of drugs in tumor tissues utilizing the enhanced permeability and retention effect and to incorporate various kinds of drugs into the inner core by chemical conjugation or physical entrapment with relatively high stability. The size of the micelles can be controlled within the diameter range of 20–100 nm, to ensure that the micelles do not pass through normal vessel walls; therefore, a reduced incidence of the side effects of the drugs may be expected due to the decreased volume of distribution. There are several anti-cancer agent-incorporated micelle carrier systems under clinical evaluation. Phase 1 studies of a cisplatin-incorporated micelle, NC-6004 and an SN-38-incorporated micelle, NK012, are now underway. A Phase 2 study of a paclitaxel-incorporated micelle, NK105, against stomach cancer is also underway.

Key words: DDS – polymer micelles – clinical trial – EPR effect

INTRODUCTION

There are two main concepts in drug delivery system (DDS), active targeting and passive targeting. Active targeting involves monoclonal antibodies or ligands to tumor-related receptors, which can target the tumor by utilizing the specific binding ability between the antibody and antigen or between the ligand and its receptor. However, the application of DDS using monoclonal antibodies is restricted to tumors expressing high levels of related antigens. The passive targeting system can be achieved by the enhanced permeability and retention (EPR) effect (1). The EPR effect is based on the pathophysiological characteristics of solid tumor tissues: hypervascularity, incomplete vascular architecture, secretion of vascular permeability factors stimulating extravasation within cancer tissue and absence of effective lymphatic drainage from tumors, which impedes the efficient clearance of macromolecules accumulated in solid tumor tissues.

Several techniques to use maximally the EPR effect have been developed, e.g. modification of drug structures and development of drug carriers. Polymeric micelle-based anti-cancer drugs were originally developed by Prof Kataoka et al. (2–4) in the late 1980s or early 1990s. Polymeric micelles were expected to increase the accumulation of drugs in tumor tissues utilizing the EPR effect and to incorporate various kinds of drugs into the inner core by chemical conjugation or physical entrapment with relatively high stability. The size of the micelles can be controlled within the diameter range of 20–100 nm, to ensure that the micelles do not pass through normal vessel walls; therefore, a reduced incidence of the adverse effects of the drugs may be expected.

In this article, polymeric micelle systems for which clinical trials are now underway are reviewed.

For reprints and all correspondence: Yasuhiro Matsumura, Investigative Treatment Division, Research Center for Innovative Oncology, National Cancer Center Hospital East, Kashiwa, Chiba, Japan. E-mail: yhmatsum@east.ncc.go.jp

NK105, PACLITAXEL-INCORPORATING MICELLAR NANOPARTICLE

Background

Paclitaxel (PTX) is one of the most useful anti-cancer agents known for various cancers, including ovarian, breast and lung cancers (5,6). However, PTX has serious adverse effects, e.g. neutropenia and peripheral sensory neuropathy. In addition, anaphylaxis and other severe hypersensitive reactions have

been reported to develop in 2–4% of patients receiving the drug even after premedication (P) with anti-allergic agents; these adverse reactions have been attributed to the mixture of Cremophor EL and ethanol which was used to solubilize PTX (7,8). Of the adverse reactions, neutropenia can be prevented or managed effectively by administering a granulocyte colony-stimulating factor. On the other hand, there are no effective therapies to prevent or to reduce nerve damage, which is associated with peripheral neuropathy caused by PTX; therefore, neurotoxicity constitutes a significant dose-limiting toxicity (DLT) of the drug (9,10).

Preclinical Study

To construct NK105 micellar nanoparticles (Fig. 1), block copolymers consisting of polyethylene glycol and polyaspartate, the so-called PEG–polyaspartate described previously (2–4,11), were used. PTX was incorporated into polymeric micelles formed by physical entrapment utilizing hydrophobic interactions between PTX and the block copolymer polyaspartate chain (12).

Pharmacokinetic study showed that NK105 exhibited slower clearance from the plasma than PTX. The plasma concentration at 5 min (C_{5min}) and the area under the curve (AUC) of NK105 were 11- to 20-fold and 50- to 86-fold higher for NK105 than that for PTX, respectively. The maximum concentration (C_{max}) and AUC of NK105 in Colon 26 tumors were ~three times and 25 times higher for NK105 than that for PTX, respectively. NK105 continued to accumulate in the tumors until 72 h after injection (12). In *in vivo* anti-tumor activity, BALB/c mice bearing s.c. HT-29 colon cancer tumors showed decreased tumor growth rates after the administration of PTX and NK105. However, NK105 exhibited superior anti-tumor activity as compared with PTX ($P < 0.001$). The anti-tumor activity of NK105 administered at a PTX-equivalent dose of 25 mg/kg was comparable to that obtained after the administration of free PTX 100 mg/kg. Tumor suppression by NK105 increased in a dose-dependent manner. Tumors disappeared after the first dosing to mice treated with NK105 at a PTX-equivalent dose of 100 mg/kg, and all mice remained tumor-free thereafter (Fig. 2). In addition, less weight loss was induced in mice

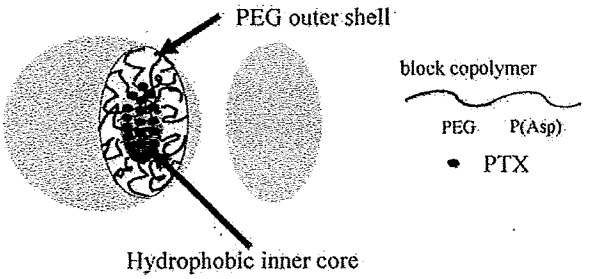

Figure 1. Preparation and characterization of NK105. The micellar structure of NK105 paclitaxel (PTX) was incorporated into the inner core of the micelle. PEG, polyethylene glycol (12).

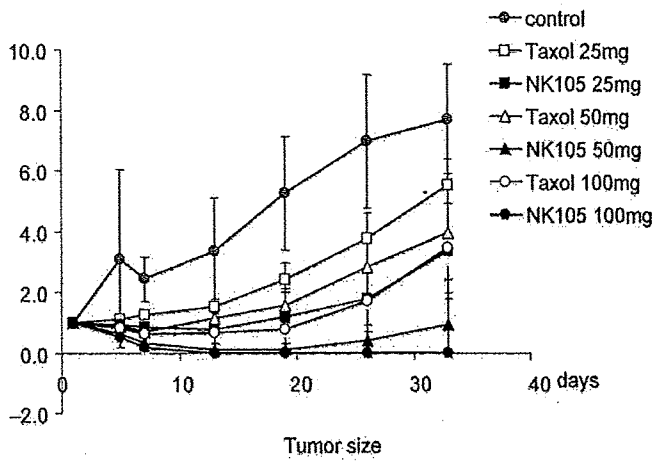

Figure 2. Effects of PTX (open symbols) and NK105 (closed symbols). PTX and NK105 were injected intravenously once weekly for 3 weeks at PTX-equivalent doses of 25 mg/kg (open square, closed square), 50 mg/kg (open triangle, closed triangle) and 100 mg/kg (open circle, closed circle), respectively. Saline was injected to control animals (open square) (12).

given NK105 100 mg/kg than in those given the same dose of free PTX (12).

Treatment with PTX has resulted in cumulative sensory-dominant peripheral neurotoxicity in humans, characterized clinically by numbness and/or paraesthesia of the extremities. Pathologically, axonal swelling, vesicular degeneration and demyelination were observed. We, therefore, examined the effects of free PTX and NK105 using both electrophysiological and morphological methods. Prior to drug administration, there were no significant differences in the amplitude of caudal sensory nerve action potential between two drug administration groups. The amplitude was significantly smaller in the PTX group than in the control group ($P < 0.01$), while the amplitude was significantly larger in the NK105 group than in the PTX group ($P < 0.05$) and was comparable between the NK105 group and the control group (Fig. 3).

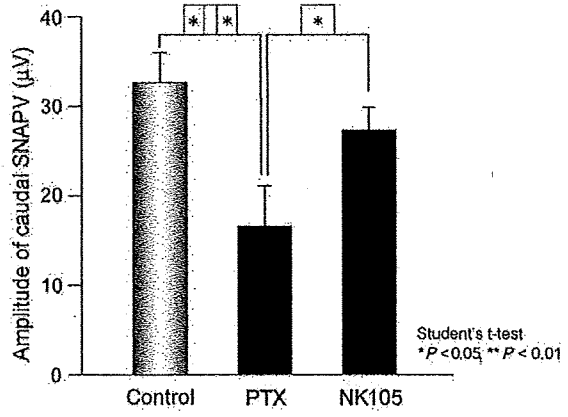

Figure 3. Effects of PTX or NK105 on the amplitude of rat caudal sensory nerve action potentials as examined 5 days after weekly injections for 6 weeks. Rats ($n = 14$) were injected with NK105 or PTX at a PTX-equivalent dose of 7.5 mg/kg. Five percent glucose was also injected in the same manner to animals in the control group (12).

Clinical Study

A Phase 1 study was designed to determine maximum tolerated dose (MTD), DLTs, the recommended dose (RD) for Phase 2 and the pharmacokinetics of NK105 (13). NK105 was administered by 1-h intravenous infusion every 3 weeks without anti-allergic P. The starting dose was 10 mg PTX-equivalent/m^2, and dose escalated according to the accelerated titration method. Nineteen patients were treated at the following doses: 10 ($n = 1$), 20 ($n = 1$), 40 ($n = 1$), 80 ($n = 1$), 110 ($n = 3$), 150 ($n = 7$) and 180 mg/m^2 ($n = 5$). Tumor types treated have included: pancreatic ($n = 11$), bile duct ($n = 5$), gastric ($n = 2$) and colon ($n = 1$). Neutropenia has been the predominant hematological toxicity and Grade 3 or 4 neutropenia was observed in patients treated at 110, 150 and 180 mg/m^2. One patient at 180 mg/m^2 developed Grade 3 fever. No other Grade 3 or 4 non-hematological toxicity including neuropathies was observed. DLTs were observed in two patients at the 180 mg/m^2 (Grade 4 neutropenia lasting for more than 5 days), which was determined as MTD. Allergic reactions were not observed in any of the patients except in one patient at 180 mg/m^2. A partial response was observed in one pancreatic cancer patient, who received more than 12 courses of NK105 (13) (Fig. 4). Despite the long-time usage, only Grade 1 or 2 neuropathy was observed by modifying the dose or period of drug administration. Colon and gastric cancer patients experienced stable disease lasting 10 and 7 courses, respectively. The C_{max} and AUC of NK105 showed dose-dependent characteristics. The plasma AUC of NK105 at 180 mg/m^2 was ~30-fold higher than that of the commonly used PTX formulation (13) (Fig. 5). DLT was Grade 4 neutropenia. NK105 generates prolonged systemic exposure to PTX in plasma. Tri-weekly 1-h infusion of NK105 was feasible and well tolerated, with anti-tumor activity in pancreatic cancer patients. A Phase 2 study of NK105 is now underway against advanced stomach cancer as a second line therapy.

NC-6004, CISPLATIN-INCORPORATING MICELLAR NANOPARTICLE

Background

Cisplatin [*cis*-dichlorodiammineplatinum (II): CDDP] is a key drug in the chemotherapy for cancers, including lung, gastrointestinal and genitourinary cancer (14,15). However, we often find that it is necessary to discontinue treatment with CDDP due to its adverse reactions, e.g. nephrotoxicity and neurotoxicity, despite its persisting effects (16). Platinum analogues, e.g. carboplatin and oxaliplatin (17), have been developed to date to overcome these CDDP-related disadvantages. Consequently, these analogues are becoming the standard drugs for ovarian (18) and colon cancers (19). However, those regimens including CDDP are considered to constitute the standard treatment for lung, stomach, testicular (20) and urothelial cancers (21). Therefore, the development of a DDS technology is anticipated, which would offer the better selective accumulation

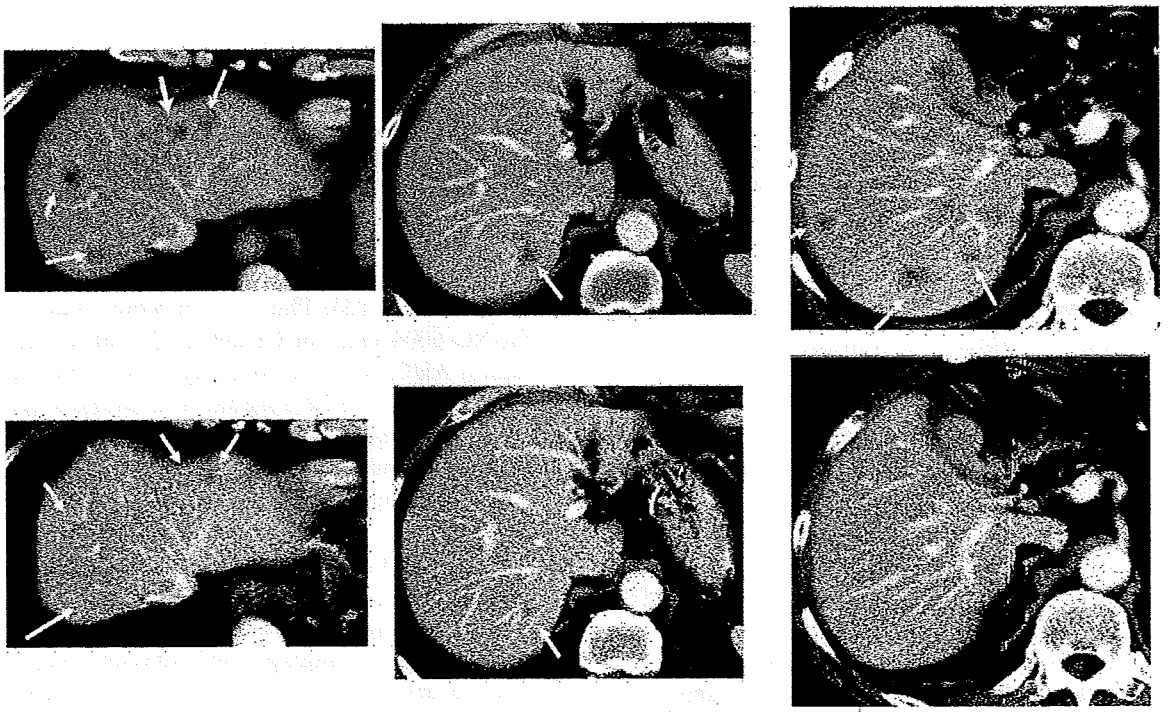

Figure 4. Serial computed tomography (CT) scans. A 60-year-old male with pancreatic cancer, who was treated with NK105 at a dose level of 150 mg/m^2. Baseline scan (upper panels) showing multiple metastasis in the liver. Partial response, characterized by a more than 90% decrease in the size of the liver metastasis (lower panels) compared with the baseline scan. The anti-tumor response was maintained for nearly 1 year (13).

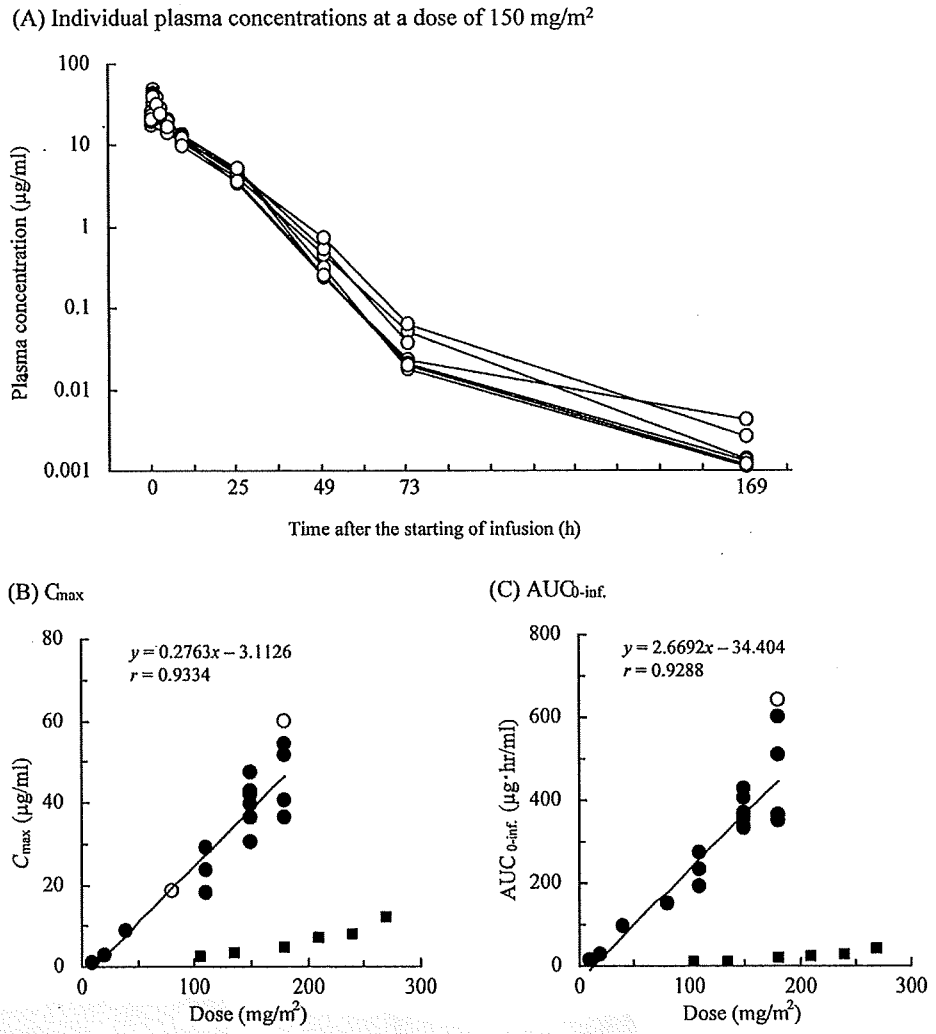

Figure 5. (A) Individual plasma concentrations of PTX in seven patients following 1 h intravenous infusion of NK105 at a dose of 150 mg/m^2. Relationships between dose and C_{max} (B), and between dose and AUC0-inf. (C) of PTX in patients following 1 h intravenous infusion of NK105. Regression analysis for dose versus C_{max} was applied using all points except for one patient at 80 mg/m^2 whose medication time became 11 min longer and one patient at 180 mg/m^2 who had medication discontinuation and steroid medication (open circle). Regression analysis for dose vs. AUC0-inf. was applied using all points except for one patient who had medication discontinuation and steroid medication (closed circle). Relationships between dose and C_{max}, and AUC0-inf in patients following conventional PTX administration were plotted (closed square) (13).

of CDDP into solid tumors while lessening its distribution into normal tissue.

Preclinical Study

NC-6004 consists of PEG, a hydrophilic chain that constitutes the outer shell of the micelles, and the coordinate complex of poly(glutamic acid) [P(Glu)] and CDDP, a polymer–metal complex-forming chain that constitutes the inner core of the micelles (22) (Fig. 6). The molecular weight of PEG-P(Glu) as a sodium salt was ~18 000 [PEG: 12 000; P(Glu): 6000]. The release rates of CDDP from NC-6004 were 19.6 and 47.8% at 24 and 96 h, respectively. In distilled water, furthermore, NC-6004 was stable without releasing cisplatin.

The AUC_{0-t} and C_{max} values were significantly higher in animals given NC-6004 than in animals given CDDP, namely, 65- and 8-fold, respectively ($P < 0.001$ and 0.001, respectively) (23). The C_{max} in tumor was 2.5-fold higher for NC-6004 than for CDDP ($P < 0.001$). Furthermore, the tumor AUC was 3.6-fold higher for NC-6004 than for CDDP (81.2 and 22.6 μg/ml h in animals given NC-6004 and CDDP, respectively) (23).

BALB/c nude mice implanted with a human gastric cancer cell line MKN-45 showed decreased tumor growth rates after i.v. injection of CDDP and NC-6004 (Fig. 7A). The NC-6004 administration groups at the same dose levels as CDDP showed no significant difference in tumor growth rate. Regarding time-course changes in body weight change rate, the CDDP 5 mg/kg administration group showed a significant decrease ($P < 0.001$) in body weight as compared with the control group. On the other hand, NC-6004 administration group did not show a decrease in body weight as compared with the control group (Fig. 7B).

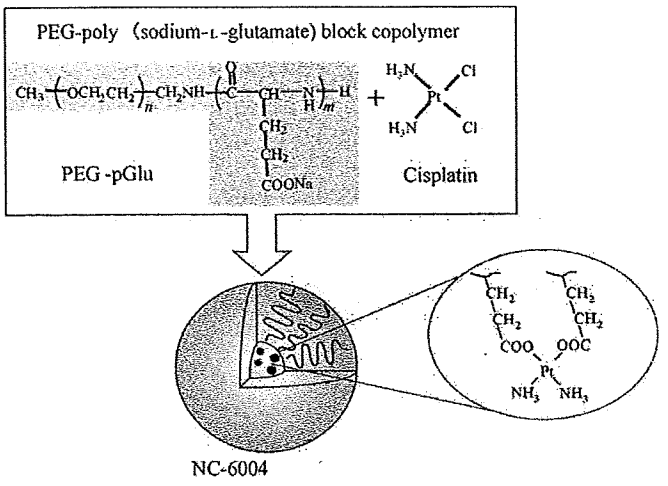

Figure 6. Preparation and characterization of cisplatin (CDDP)-incorporating polymeric micelles (NC-6004). Chemical structures of CDDP and polyethylene glycol poly(glutamic acid) block copolymers [PEG-P(Glu) block copolymers], and the micellar structures of CDDP-incorporating polymeric micelles (NC-6004) (22).

Regarding toxicity, the CDDP 10 mg/kg administration group showed significantly higher plasma concentrations of blood urea nitrogen and creatinine as compared with the control group ($P < 0.05$ and 0.001, respectively), with the NC-6004 10 mg/kg administration group ($P < 0.05$ and 0.001, respectively) (Fig. 8A and B). Light microscopy indicated tubular dilation with flattening of the lining cells of the tubular epithelium in the kidney from all animals in the CDDP 10 mg/kg administration group. On the other hand, no histopathologic change was observed in the kidneys from all animals in the NC-6004 10 mg/kg administration group (data not shown). Animals given NC-6004 showed no delay in sensory nerve condition velocities (SNCVs) as compared with animals given 5% glucose. On the other hand, animals given CDDP showed a significant delay ($P < 0.05$) in SNCV as compared with animals given NC-6004 (Fig. 9A). The analysis by ICP-MS on sciatic nerve concentrations of platinum showed that the concentrations were significantly ($P < 0.05$) lower in animals given NC-6004 (Fig. 9B). This finding is believed to be a factor that reduced neurotoxicity following NC-6004 administration as compared with the CDDP administration (23).

Clinical Study

A Phase 1 trial was run in two UK experimental cancer medicine centers with the PK assays performed in a good laboratory practice-accredited laboratory in Newcastle University (24).

Patients with solid tumors were included in this open-label trial. Usual Phase 1 inclusion and exclusion criteria were applied, including adequate renal function. Patients were limited to one previous course of platinum-based treatment with maximum dose limits of cisplatin, carboplatin or oxaliplatin.

Dose escalation proceeded in two stages. In Stage 1, we recruited cohorts of one to three patients until Grade 2 toxicity was seen in Cycle 1. In Stage 2, we had cohorts of three patients expanding to six if one of three DLT and to confirm MTD.

The starting dose for the Phase 1 study was 10 mg/m^2. NC-6004 was administered as a 60 min infusion with a total infusion volume of 500 ml. Treatment was repeated on a 3-weekly cycle until progressive disease, intolerance of the agent or patient withdrawal. Pharmacokinetic analysis of total plasma platinum (Pt), micellar Pt and ultrafiltrate Pt (UF Pt) was performed using WinNonlin version 1.3 to calculate C_{max}, T_{max}, half-life and AUC for all Pt species. Clearance and volume of distribution were calculated based on the measurements of total and micellar Pt.

In this trial, 17 patients (10 male, 7 female) were treated. The median age (range) was 59 years (40–80), and tumor

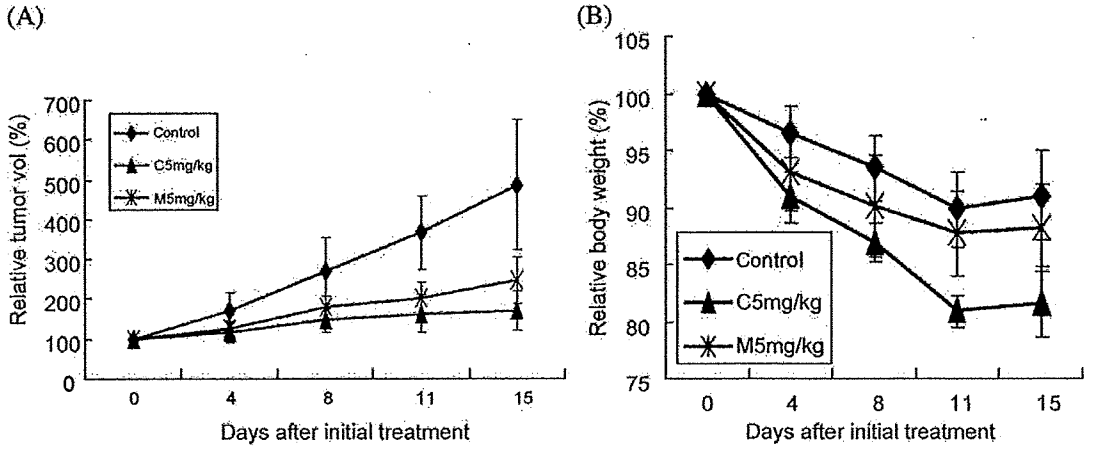

Figure 7. Relative changes in MKN-45 tumor growth rates in nude mice. (A) CDDP (closed triangle) and NC-6004 (cross symbol) were injected intravenously every 3 days, three administrations in total, at CDDP-equivalent doses of 5 mg/kg. Five percent glucose was injected in the control mice (open diamond). (B) Changes in relative body weight. Data were derived from the same mice as those used in the present study. Values are expressed as the mean ± SE (23).

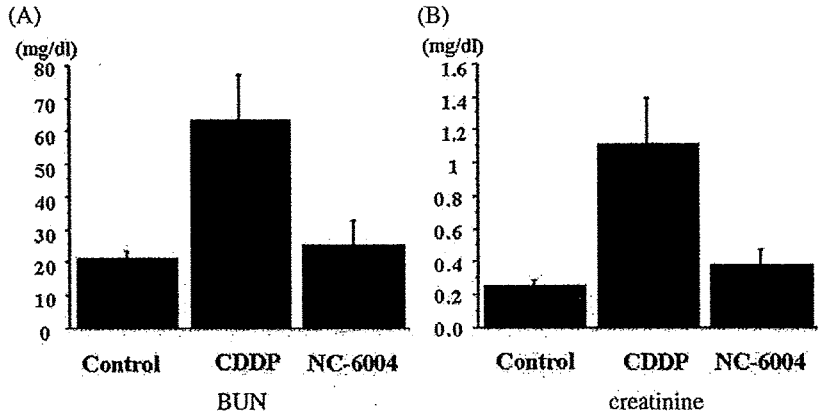

Figure 8. Nephrotoxicity of CDDP and NC-6004. Plasma concentrations of blood urea nitrogen (BUN) and creatinine were measured after a single i.v. injection of 5% glucose ($n = 8$), CDDP at a dose of 10 mg/kg ($n = 12$), NC-6004 at a dose of 10 mg/kg ($n = 13$) on a CDDP basis (23).

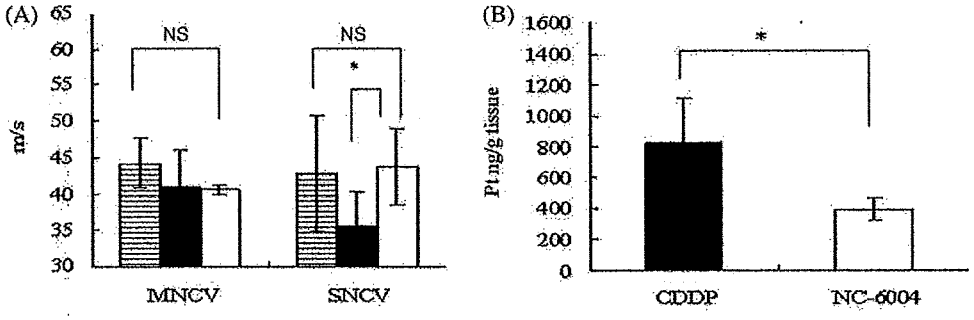

Figure 9. Neurotoxicity of CDDP and NC-6004 in rats. Rats ($n = 5$) were given CDDP (2 mg/kg), NC-6004 (an equivalent dose of 2 mg/kg CDDP), or 5% glucose, all intravenously twice a week, 11 administrations in total. Sensory nerve conduction velocity and motor nerve conduction velocity of the sciatic nerve at Week 6 after the initial administration (A). The platinum concentration in the sciatic nerve. Rats were given CDDP (5 mg/kg, $n = 5$), NC-6004 (an equivalent dose of 5 mg/kg CDDP, $n = 5$) or 5% glucose ($n = 2$), all intravenously twice a week, four administrations in total. On Day 3 after the final administration, a segment of the sciatic nerve was removed and the platinum concentration in the sciatic nerve was measured by ICP-MS (B). The data are expressed as the mean ± SD. $^*P < 0.05$ (23).

types included colorectal (4), NSCLC (3), esophageal (2), pancreatic (2), melanoma (2) and one each of GIST, mesothelioma, renal cell and hepatocellular cancer. Treatment was well tolerated with little nausea (no routine use of prophylactic antiemetics) and no protocol-defined DLTs were observed. There was no myelotoxicity or neurotoxicity and no changes in audiometry (Table 1).

A Grade 2 fall in ethylenediamine tetraacetic acid (EDTA) glomerular filtration rate (GFR) was observed at 40 mg/m^2, and post-hydration (H) with 1L N saline IV over 30 min for all patients was therefore instituted and followed by administration of doses up to 120 mg/m^2 without significant nephrotoxicity. Four hypersensitivity reactions occurred in the first nine patients on or after Cycle 2. After introduction of P with anti-histamines and corticosteroids, two further reactions were seen, during the third or fourth cycle. Three patients had previous platinum exposure, and three were platinum-naïve (Table 1).

The best response was stable disease and this was seen in seven of 17 (41%) patients.

In the ultrafiltrate fraction, there was delayed ($T_{max} =$ 24 h) and prolonged (half-life 68–580 h) detection of small molecular weight platinum species. NC-6004 provides a sustained release of potentially active platinum species. Using gel-filtration, we have been able to separate the Pt present in the original formulation from other Pt species in the plasma. The kinetics of UF Pt indicated a delayed and sustained release of cisplatin after dosing with NC-6004.

This novel formulation of cisplatin is well tolerated with minimal nephrotoxicity and no significant myelosuppression, emesis or neurotoxicity but a higher rate of hypersensitivity reactions than predicted. Disease stabilization has been seen in heavily pre-treated patients with efficacy best assessed in future Phase 2 trials. The recommended Phase 2 dose of NC-6004 for monotherapy is 90–120 mg/m^2 and for the combination is 60–90 mg/m^2.

NK012, SN-38-INCORPORATING MICELLAR NANOPARTICLE

Background

The anti-tumor plant alkaloid camptothecin (CPT) is a broad-spectrum anti-cancer agent that targets the DNA

Table 1. Patient results of NC-6004 Phase 1 trial

Dose level (mg/m^2)	No of patients	No of cycles (median)	Renal impairment	EDTA GFR change (ml/min)	Hypersensitivity (cycle)	Best response
1 (10)	1	3			Gr 2 (C3)	SD
2 (20)	1	2				PD
3 (40)	3	1–4 (2)	Gr 2 (C1)	95 → 39		1 SD
						2 PD
4 (60)	3	2 (2)			Gr 1 (C2)	1 NE
+ H					Gr 3 (C2)	2 PD
5 (90)	6	2–4 (2)	Gr 2 (C1)	74 → 59	Gr 3 (C4)	3 SD
+H			Gr 2 (C2)	67 → 53		3 PD
6 (120)	3	2–4 (3)			Gr 2 (C4)	2 SD
+ H + P					Gr 3 (C3)	1 PD

A Grade 2 fall in EDTA GFR was observed at 40 mg/m^2 and hydration with 1000 ml saline i.v. over 30 mm for all patients was therefore instituted and following this administration of doses up to 120 mg/m^2 without significant nephrotoxicity was performed (24). EDTA, ethylenediamine tetraacetic acid; GFR, glomerular filtration rate; Gr, grade; C, cycle; SD, standard deviationl; PD, progressive disease; NE, not evaluated.

topoisomerase I. Although CPT has showed promising anti-tumor activity *in vitro* and *in vivo* (25,26), it has not been used clinically because of its low therapeutic efficacy and severe toxicity (27,28). Among CPT analogs, irinotecan hydrochloride (CPT-11) has recently been demonstrated to be active against colorectal, lung and ovarian cancers (29–33). CPT-11 itself is a prodrug and is converted to 7-ethyl-10-hydroxy-CPT (SN-38), a biologically active metabolite of CPT-11, by carboxylesterases (CEs). SN-38 exhibits up to 1000-fold more potent cytotoxic activity against various cancer cells *in vitro* than CPT-11 (34). Although CPT-11 is converted to SN-38 in the liver and tumor, the metabolic conversion rate is <10% of the original volume of CPT-11 (35,36). In addition, the conversion of CPT-11 to SN-38 depends on the genetic inter-individual variability of CE activity (37). Thus, the direct use of SN-38 might be of great advantage, and attractive, for cancer treatment. For the clinical use of SN-38, however, it is essential to develop a soluble form of water-insoluble SN-38. The progress of the manufacturing technology of 'micellar nanoparticles' may make it possible to utilize SN-38 for *in vivo* experiments and further clinical use.

Preclinical Study

SN-38 was bound to the carboxylic acid on a polyglutamate (PGlu) chain of block copolymer through the ester bond. NK012 is an SN-38-loaded polymeric micelle constructed in an aqueous milieu by the self-assembly of an amphiphilic block copolymer, PEG–PGlu(SN-38) (38) (Fig. 10). The mean particle size of NK012 is 20 nm in diameter with a relatively narrow range. The releasing rates of SN-38 from NK012 in phosphate-buffered saline at 37°C were 57 and 74% at 24 and 48 h, respectively, and that in 5% glucose solution at 37°C were 1 and 3% at 24 and 48 h, respectively. These results indicate that NK012 can release SN-38 under neutral conditions even without the presence of a hydrolytic enzyme and is stable in 5% glucose solution. It is suggested that NK012 is stable before administration and starts to release SN-38, the active component, under physiological conditions after administration.

In PK study, after injection of CPT-11, the concentrations of CPT-11 and SN-38 for plasma declined rapidly with time in a log-linear fashion. On the other hand, NK012 (polymer-bound SN-38) exhibited slower clearance. The clearance of NK012 in the HT-29 tumor was significantly slower and the concentration of free SN-38 was maintained at >30 ng/g even at 168 h after injection. Anti-tumor activity of NK012 was evaluated in lung (38), renal (39), pancreatic (40) and stomach cancers xenografts (41) in comparison with CPT-11. NK012 exhibited superior anti-tumor activity in all tumors tested compared with CPT-11. Also, the therapeutic effect of NK012/5FU was significantly superior to that of CPT-11/5FU against the HT-29 xenografts ($P = 0.0004$). A 100% CR rate was obtained in the NK012/5FU group, as compared with the 0% CR rate in the CPT-11/5FU (Fig. 11) (42).

It may be concluded that NK012 can selectively accumulate in any tumor xenografts, to be distributed effectively throughout the entire body of the tumor, including in hypovascular tumors, and show sustained-release for a prolonged period of time. Consequently, NK012 can exert more significant anti-tumor activity as compared with CPT-11, which is not an ideal formulation for realizing the time-dependent actions of the drug (40).

Clinical Study

Two independent Phase 1 studies of NK012 have been almost completed in the National Cancer Center in Japan (43) and the Sarah Canon Cancer Center in the USA (44) in patients with advanced solid tumors to determine the

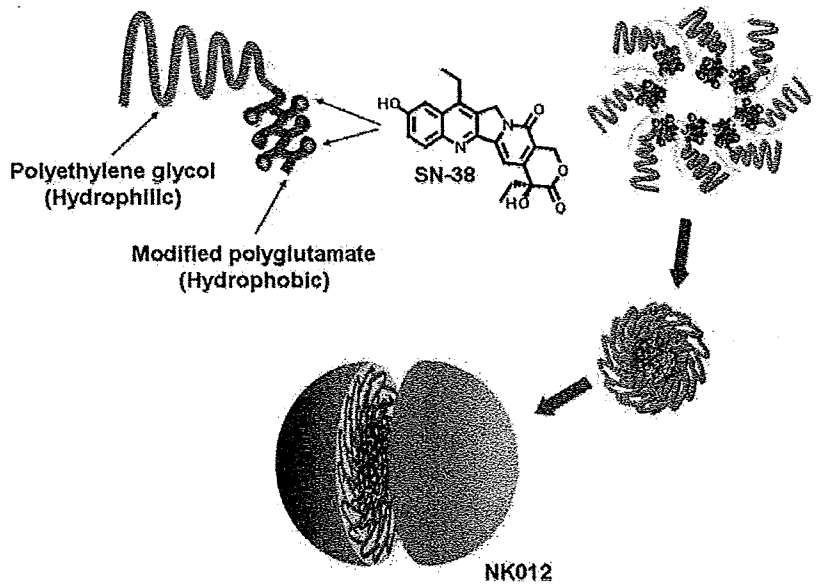

Figure 10. Schematic structure of NK012. A polymeric micelle carrier of NK012 consists of a block copolymer of PEG (molecular weight of ~5000) and partially modified polyglutamate (~20 U). Polyethylene glycol (hydrophilic) is believed to be the outer shell and SN-38 was incorporated into the inner core of the micelle (38).

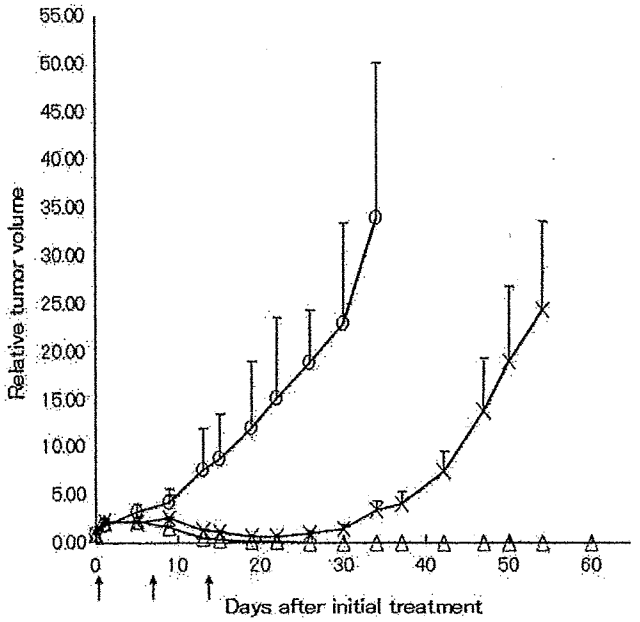

Figure 11. Effect of NK012/5-FU as compared with that of CPT-11/5-FU against HT-29 tumor-bearing mice. (Open circle) control, (cross symbol) CPT-11 50 mg/kg 24 h before 5-FU 50 mg/kg, (closed triangle) NK012 10 mg/kg 24 h before 5-FU 50 mg/kg (42).

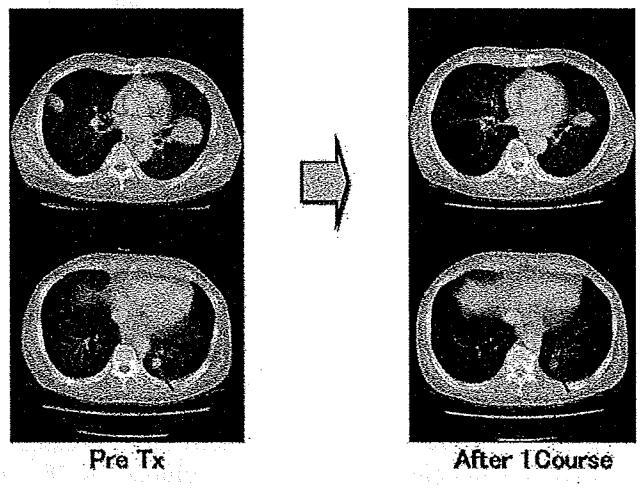

Figure 12. CT scan of an esophageal cancer patient with lung metastasis. This patient had previously undergone 5-FU+CDDP followed by taxotere. Partial response, characterized by a more than 50% decrease in size of the lung metastasis compared with the baseline scan (43).

pharmacokinetics, toxicity profile and the RD for Phase 2 of NK012. NK012 is infused intravenously over 30 min every 21 days until disease progression or unacceptable toxicity occurs. UGT1A1 genotype screening was performed prior to enrollment, and UGT1A1*28/*28 homozygotes were treated at a reduced dose level with the potential for dose escalation based on toxicities. In a Japanese study, the starting dose was 2 mg/m^2 as an SN-38 equivalent, and the dose was escalated by the accelerated titration method. In an US study, the starting dose was 9 mg/m^2 as an SN-38 equivalent and at least three patients were treated at each dose level.

DLT was determined to be neutropenia. MTD will become >28 mg/m^2 and RD may become ≤28 mg/m^2. Non-hematological toxicities including diarrhea were mostly less than Grade 2 in Course 1. One partial response has been reported in a patient with esophageal cancer in a Japanese study (Fig. 12), and three patients with triple negative breast cancer and one patient with small cell lung cancer had PR in the US study. In conclusion, NK012 is well tolerated and has demonstrated anti-tumor activity in patients with refractory tumors.

CONCLUSION

A quarter of a century has passed since the EPR effect was discovered. Until recently, the EPR had not been recognized in the field of oncology. However, many oncologists have now become acquainted with it, since some drugs such as doxil, abraxane and several PEGylated proteinacious agents formulated based on the EPR have been approved in the field of oncology. Micelle carrier systems described in this article are obviously categorized as DDS based on the EPR. It is expected that some anti-cancer agents incorporating micelle nanoparticles may be approved for clinical use soon.

Our next task is to develop DDS, which can accumulate selectively in solid tumors but also allow distribution of the delivered bullets (anti-cancer agents) through the entire mass of the solid tumor tissue.

Funding

This work was supported partly by a Grant-in-Aid from the 3rd Term Comprehensive Control Research for Cancer, Ministry of Health, Labor and Welfare (Y. Matsumura) and Scientific Research on Priority Areas from the Ministry of Education, Culture, Sports, Science and Technology (Y. Matsumura), and the Princess Takamatsu Cancer Research Fund (Y. Matsumura).

Conflict of interest statement

None declared.

References

1. Matsumura Y, Maeda H. A new concept for macromolecular therapeutics in cancer chemotherapy: mechanism of tumoritropic accumulation of proteins and the antitumor agent smancs. *Cancer Res* 1986;46:6387–92.
2. Kataoka K, Kwon GS, Yokoyama M, Okano T, Sakurai Y. Block copolymer micelles as vehicles for drug delivery. *J Controlled Release* 1993;24:119–32.
3. Yokoyama M, Miyauchi M, Yamada N, Okano T, Sakurai Y, Kataoka K, et al. Polymer micelles as novel drug carrier: adriamycin-conjugated poly(ethylene glycol)-poly(aspartic acid) block copolymer. *J Controlled Release* 1990;11:269–78.
4. Yokoyama M, Okano T, Sakurai Y, Ekimoto H, Shibazaki C, Kataoka K. Toxicity and antitumor activity against solid tumors of micelle-forming polymeric anticancer drug and its extremely long circulation in blood. *Cancer Res* 1991;51:3229–36.
5. Khayat D, Antoine EC, Coeffic D. Taxol in the management of cancers of the breast and the ovary. *Cancer Invest* 2000;18:242–60.
6. Carney DN. Chemotherapy in the management of patients with inoperable non-small cell lung cancer. *Semin Oncol* 1996;23:71–5.
7. Weiss RB, Donehower RC, Wiernik PH, Ohnuma T, Gralla RJ, Trump DL, et al. Hypersensitivity reactions from taxol. *J Clin Oncol* 1990;8:1263–8.
8. Rowinsky EK, Donehower RC. Paclitaxel (taxol). *N Engl J Med* 1995;332:1004–14.
9. Rowinsky EK, Chaudhry V, Forastiere AA, Sartorius SE, Ettinger DS, Grochow LB, et al. Phase I and pharmacologic study of paclitaxel and cisplatin with granulocyte colony-stimulating factor: neuromuscular toxicity is dose-limiting. *J Clin Oncol* 1993;11: 2010–20.
10. Wasserheit C, Frazein A, Oratz R, Sorich J, Downey A, Hochster H, et al. Phase II trial of paclitaxel and cisplatin in women with advanced breast cancer: an active regimen with limiting neurotoxicity. *J Clin Oncol* 1996;14:1993–9.
11. Yokoyama M, Okano T, Sakurai Y, Ekimoto H, Shibazaki C, Kataoka K. Toxicity and antitumor activity against solid tumors of micelle-forming polymeric anticancer drug and its extremely long circulation in blood. *Cancer Res* 1991;51:3229–36.
12. Hamaguchi T, Matsumura Y, Suzuki M, Shimizu K, Goda R, Nakamura I, et al. NK105, a paclitaxel-incorporating micellar nanoparticle formulation, can extend in vivo antitumour activity and reduce the neurotoxicity of paclitaxel. *Brit J Cancer* 2005;92:1240–6.
13. Hamaguchi T, Kato K, Yasui H, Morizane C, Ikeda M, Ueno H, et al. A Phase I and Pharmacokinetic Study of NK105, a paclitaxel-incorporating micellar nanoparticle formulation. *Brit J Cancer* 2007;97:170–6.
14. Horwich A, Sleijfer DT, Fossa SD, Kaye SB, Oliver RT, Cullen MH, et al. Randomized trial of bleomycin, etoposide, and cisplatin compared with bleomycin, etoposide, and carboplatin in good-prognosis metastatic nonseminomatous germ cell cancer: a Multiinstitutional Medical Research Council/European Organization for Research and Treatment of Cancer Trial. *J Clin Oncol* 1997;15:1844–52.
15. Roth BJ. Chemotherapy for advanced bladder cancer. *Semin Oncol* 1996;23:633–44.
16. Pinzani V, Bressolle F, Haug IJ, Galtier M, Blayac JP, Balmes P. Cisplatin-induced renal toxicity and toxicity-modulating strategies: a review. *Cancer Chemother Pharmacol* 1994;35:1–9.
17. Cleare MJ, Hydes PC, Malerbi BW, Watkins DM. Anti-tumor platinum complexes: relationships between chemical properties and activity. *Biochimie* 1978;60:835–50.
18. du Bois A, Luck HJ, Meier W, Adams HP, Mobus V, Costa S, et al. A randomized clinical trial of cisplatin/paclitaxel versus carboplatin/paclitaxel as first-line treatment of ovarian cancer. *J Natl Cancer Inst* 2003;95:1320–9.
19. Cassidy J, Tabernero J, Twelves C, Brunet R, Butts C, Conroy T, et al. XELOX (capecitabine plus oxaliplatin): active first-line therapy for patients with metastatic colorectal cancer. *J Clin Oncol* 2004;22: 2084–91.
20. Horwich A, Sleijfer DT, Fossa SD, Kaye SB, Oliver RT, Cullen MH, et al. Randomized trial of bleomycin, etoposide, and cisplatin compared with bleomycin, etoposide, and carboplatin in good-prognosis metastatic nonseminomatous germ cell cancer: a Multiinstitutional Medical Research Council/European Organization for Research and Treatment of Cancer Trial. *J Clin Oncol* 1997;15:1844–52.
21. Bellmunt J, Ribas A, Eres N, Albanell J, Almanza C, Bermejo B, et al. Carboplatin-based versus cisplatin-based chemotherapy in the treatment of surgically incurable advanced bladder carcinoma. *Cancer* 1997;80: 1966–72.
22. Nishiyama N, Okazaki S, Cabral H, Miyamoto M, Kato Y, Sugiyama Y, et al. Novel cisplatin-incorporated polymeric micelles can eradicate solid tumors in mice. *Cancer Res* 2003;63:8977–83.
23. Uchino H, Matsumura Y, Negishi T, Hayashi T, Honda T, Nishiyama N, et al. Cisplatin-incorporating polymeric micelles (NC-6004) can reduce nephrotoxicity and neurotoxicity of cisplatin in rats. *Brit J Cancer* 2005;93:678–87.
24. Wilson RH, Plummer R, Adam J, Eatock MM, Boddy AV, Griffin M, et al. Phase I and pharmacokinetic study of NC-6004, a new platinum entity of cisplatin-conjugated polymer forming micelles. *Am Soc Clin Oncol* 2008; (Abs# 2573).
25. Li LH, Fraser TJ, Olin EJ, Bhuyan BK. Action of camptothecin on mammalian cells in culture. *Cancer Res* 1972;32:2643–50.
26. Gallo RC, Whang-Peng J, Adamson RH. Studies on the antitumor activity, mechanism of action, and cell cycle effects of camptothecin. *J Natl Cancer Inst* 1971;46:789–95.
27. Gottlieb JA, Guarino AM, Call JB, Oliverio VT, Block JB. Preliminary pharmacologic and clinical evaluation of camptothecin sodium (NSC-100880). *Cancer Chemother Rep* 1970;54:461–70.
28. Muggia FM, Creaven PJ, Hansen HH, Cohen MH, Selawry OS. Phase I clinical trial of weekly and daily treatment with camptothecin (NSC-100880): correlation with preclinical studies. *Cancer Chemother Rep* 1972;56:515–21.
29. Cunningham D, Pyrhonen S, James RD, Punt CJ, Hickish TF, Heikkila R, et al. Randomised trial of irinotecan plus supportive care versus supportive

care alone after fluorouracil failure for patients with metastatic colorectal cancer. *Lancet* 1998;352:1413–8.
30. Saltz LB, Cox JV, Blanke C, Rosen LS, Fehrenbacher L, Moore MJ, et al. Irinotecan plus fluorouracil and leucovorin for metastatic colorectal cancer. Irinotecan Study Group. *N Engl J Med* 2000;343: 905–14.
31. Noda K, Nishiwaki Y, Kawahara M, Negoro S, Sugiura T, Yokoyama A, et al. Irinotecan plus cisplatin compared with etoposide plus cisplatin for extensive small-cell lung cancer. *N Engl J Med* 2002;346:85–91.
32. Negoro S, Masuda N, Takada Y, Sugiura T, Kudoh S, Katakami N, et al., CPT-11 Lung Cancer Study Group West. Randomised phase III trial of irinotecan combined with cisplatin for advanced non-small-cell lung cancer. *Br J Cancer* 2003;88:335–41.
33. Bodurka DC, Levenback C, Wolf JK, Gano J, Wharton JT, Kavanagh JJ, et al. Phase II trial of irinotecan in patients with metastatic epithelial ovarian cancer or peritoneal cancer. *J Clin Oncol* 2003;21:291–7.
34. Takimoto CH, Arbuck SG. Topoisomerase I targeting agents: the camptothecins. In: Chabner BA, Lango DL editors. Cancer Chemotherapy and Biotherapy: Principal and Practice, 3rd edn. Philadelphia (PA): Lippincott Williams & Wilkins 2001;579–646.
35. Slatter JG, Schaaf LJ, Sams JP, Feenstra KL, Johnson MG, Bombardt PA, et al. Pharmacokinetics, metabolism, and excretion of irinotecan (CPT-11) following I.V. infusion of [(14)C]CPT-11 in cancer patients. *Drug Metab Dispos* 2000;28: 423–33.
36. Rothenberg ML, Kuhn JG, Burris HA, 3rd, Nelson J, Eckardt JR, Tristan-Morales M, et al. Phase I and pharmacokinetic trial of weekly CPT-11. *J Clin Oncol* 1993;11:2194–204.
37. Guichard S, Terret C, Hennebelle I, Lochon I, Chevreau P, Fretigny E, et al. CPT-11 converting carboxylesterase and topoisomerase activities in tumor and normal colon and liver tissues. *Br J Cancer* 1999;80: 364–70.
38. Koizumi F, Kitagawa M, Negishi T, et al. Novel SN-38-incorporating polymeric micelles, NK012, eradicate vascular endothelial growth factor-secreting bulky tumors. *Cancer Res* 2006;66:10048–56.
39. Sumitomo M, Koizumi F, Asano T, Horiguchi A, Ito K, Asano T, et al. Novel SN-38-incorparated polymeric micelles, NK012, strongly suppress renal cancer progression. *Cancer Res* 2008;122:2148–53.
40. Saito Y, Yasunaga M, Kuroda J, Koga Y, Matsumura Y. Enhanced distribution of NK012 and prolonged sustained-release of SN-38 within tumors are the key strategic point for a hypovascular tumor. *Cancer Sci* 2008;99:1258–64.
41. Nakajima-Eguchi T, Yanagihara K, Takigahara M, Yasunaga M, Kato K, Hamaguchi T, et al. Antitumor effect of SN-38-releasing polymeric micelles, NK012, on spontaneous peritoneal metastases from orthotopic gastoric cancer in mice compared with irinotecan. *Cancer Res* 2008 (in press).
42. Nakajima T, Yasunaga M, kano Y, Koizumi F, Kato K, Hamaguchi T, et al. Synergistic antitumor activity of the novel SN-38 incorporating polymeric micelles, NK012, combined with 5-fluorouracil in a mouse model of colorectal cancer, as compared with that of irinotecan plus 5-fluorouracil. *Int J Cancer* 2008;122:22148–53.
43. Kato K, Hamaguchi T, Shirao K, Shimada Y, Yamada Y, Doi T, et al. Phase I study of NK012, polymer micelle SN-38, in patients with advanced cancer. *Am Soc Clin Oncol GI* 2008; (Abs#485).
44. Burris HA, III, Infante JR, Spigel DR, Greco FA, Thompson DS, Matsumoto S, et al. A phase I dose-escalation study of NK012. *Am Soc Clin Oncol* 2008; (Abs#2538).

Available online at www.sciencedirect.com
ScienceDirect
Advanced Drug Delivery Reviews 60 (2008) 899–914
Advanced DRUG DELIVERY Reviews
www.elsevier.com/locate/addr

Poly (amino acid) micelle nanocarriers in preclinical and clinical studies ☆

Yasuhiro Matsumura *

Investigative Treatment Division, Research Center for Innovative Oncology, National Cancer Center Hospital East, 6-5-1 Kashiwanoha, Kashiwa City, 277-8577 Japan

Received 18 May 2007; accepted 15 November 2007
Available online 9 February 2008

Abstract

Polymeric micelles are expected to increase the accumulation of drugs in tumor tissues utilizing the EPR effect and to incorporate various kinds of drugs into the inner core by chemical conjugation or physical entrapment with relatively high stability. The size of the micelles can be controlled within the diameter range of 20 to 100 nm, to ensure that the micelles do not pass through normal vessel walls; therefore, a reduced incidence of the side effects of the drugs may be expected due to the decreased volume of distribution.

These are several anticancer agent-incorporated micelle carrier systems under clinical evaluation. Phase 1 studies of a CDDP incorporated micelle, Nc-6004, and an sN-38 incorporated micelle, NK012, are now underway. A phase 2 study of a PTX incorporated micelle, NK105, against stomach cancer is also underway.

Keywords: Poly (amino acid) micelle nanocarrier; Drug delivery system; EPR effect; Clinical trial

Contents

☆ This review is part of the *Advanced Drug Delivery Reviews* theme issue on "Clinical Developments in Drug Delivery Nanotechnology".

* Tel./fax: 81 4 7134 6857.

0169-409X/$ - see front matter © 2008 Elsevier B.V. All rights reserved.
doi:10.1016/j.addr.2007.11.010

1. Preface

Drug delivery system (DDS) could be used for active or passive targeting of tumor tissues. The former refers to the development of monoclonal antibodies directed against tumor-related molecules that allow targeting of the tumor, because of specific binding between the antibody and its antigen. However, the application of DDS using monoclonal antibodies is restricted to tumors expressing high levels of related antigens.

Passive targeting is based on the enhanced permeability and retention (EPR) effect [1]. The EPR effect is based on the pathophysiological characteristics of solid tumor tissues: hypervascularity, incomplete vascular architecture, secretion of vascular permeability factors stimulating extravasation within cancer tissue, and absence of effective lymphatic drainage from tumors that impedes the efficient clearance of macromolecules accumulated in solid tumor tissues.

Several techniques to maximally use the EPR effect have been developed, e.g., modification of drug structures and development of drug carriers. Polymeric micelle-based anticancer drugs were originally developed by Prof. Kataoka et al. in late the 1980s or early 1990s [2–4]. Polymeric micelles were expected to increase the accumulation of drugs in tumor tissues utilizing the EPR effect and to incorporate various kinds of drugs into the inner core by chemical conjugation or physical entrapment with relatively high stability. The size of the micelles can be controlled within the diameter range of 20 to 100 nm, to ensure that the micelles do not pass through normal vessel walls; therefore, a reduced incidence of the side effects of the drugs may be expected due to the decreased volume of distribution.

In this chapter, polymeric micelle systems for which clinical trials are now underway are reviewed.

2. NK105, paclitaxel-incorporating micellar nanoparticle

Paclitaxel(PTX) is one of the most useful anticancer agents known for various cancers, including ovarian, breast, and lung cancers [5,6]. However, PTX has serious adverse effects, e.g., neutropenia and peripheral sensory neuropathy. In addition, anaphylaxis and other severe hypersensitive reactions have been reported to develop in 2–4% of patients receiving the drug even after premedication with antiallergic agents; these adverse reactions have been attributed to the mixture of Cremophor EL and ethanol which was used to solubilize PTX [7,8]. Of the adverse reactions, neutropenia can be prevented or managed effectively by administering a granulocyte colony-stimulating factor. On the other hand, there are no effective therapies to prevent or reduce nerve damage which is associated with peripheral neuropathy caused by PTX; therefore, neurotoxicity constitutes a significant dose-limiting toxicity of the drug [9,10].

2.1. Preparation and characterization of NK105

To construct NK105 micellar nanoparticles (Fig. 1), block copolymers consisting of polyethylene glycol and polyaspartate, so-called PEG-polyaspartate described previously [2–4,11], were used. PTX was incorporated into polymeric micelles formed by physical entrapment utilizing hydrophobic interactions between PTX and the block copolymer polyaspartate chain. After screening of many candidate substances, 4-phenyl-1-butanol was employed for the chemical modification of the polyaspartate block to increase its hydrophobicity. Treating with a condensing agent, 1,3-diisopropylcarbodiimide, the half of carboxyl groups on the polyaspartate were esterified with 4-phenyl-1-butanol. Molecular weight of the polymers was determined to be approximately 20,000, (PEG block: 12,000; modified polyaspartate block: 8000). NK105 was prepared by facilitating the self-association of NK105 polymers and PTX. NK105 was obtained as a freeze-dried formulation and contained ca. 23% (w/w) of PTX, as determined by reversed-phase liquid-chromatography using an ODS column with mobile

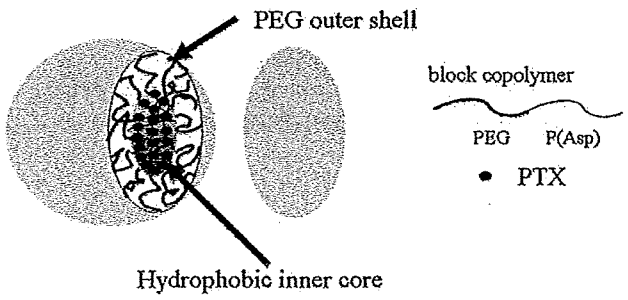

Fig. 1. Preparation and characterization of NK105. The micellar structure of NK105 PTX was incorporated into the inner core of the micelle [29].

Table 1
Pharmacokinetic parameters for the plasma and tumor concentrations of paclitaxel after single intravenous administration of NK105 and PTX to colon 26-bearing CDF1 mice

	Treatment	Dose (mg/kg)	$C_{5\ min}$ (μg/mL)	$t_{1/2z}$ (h)	AUC_{0-t} (μg·h/mL)	AUC_{0-inf} (μg·h/mL)	CL_{tot} (mL/h/kg)	V_{ss} (mL/kg)
Plasma	PTX	50	59.32	0.98	90.2[a)]	91.3	547.6	684.6
	PTX	100	157.67	1.84	309.0[b)]	309.0	323.6	812.2
	NK105	50	1157.03	5.99	7860.9[c)]	7862.3	6.4	46.4
	NK105	100	1812.37	6.82	15565.7[c)]	15573.6	6.4	54.8
			C_{max} (μg/mL)	T_{max} (h)	$t_{1/2z}$ (h)	AUC_{0-t} (μg·h/mL)		AUC_{0-inf} (μg·h/mL)
Tumor	PTX	50	12.50	2.0	7.02	120.8[b)]		133.0
	PTX	100	28.57	0.5	8.06	330.4[c)]		331.0
	NK105	50	42.45	24.0	35.07	2360.1[c)]		3192.0
	NK105	100	71.09	6.0	73.66	3884.9[c)]		7964.5

a) $AUC_{0-6\ h}$; b) $AUC_{0-24\ h}$; c) $AUC_{0-72\ h}$.
Parameters were calculated from the mean value of three or two mice by noncompartmental analysis [12].

phase consisting of acetonitrile and water (9:11, v/v) and detection of ultraviolet absorbance at 227 nm. Finally, NK105, a PTX-incorporating polymeric micellar nanoparticle formulation with a single and narrow size distribution, was obtained. The weight-average diameter of the nanoparticles was approximately 85 nm ranging from 20 to 430 nm [12].

2.2. Pharmacokinetics and pharmacodynamics of NK105

Colon 26-bearing CDF1 mice were given a single i.v. injection of PTX 50 or 100 mg/kg, or of NK105 at an equivalent dose of PTX. Subsequently, the time-course changes in the plasma and tumor levels of PTX were determined in the PTX and NK105 administration groups ; furthermore, the pharmacokinetic parameters of each group were also determined (Table 1). NK105 exhibited slower clearance from the plasma than PTX, while NK105 was present in the plasma for up to 72 h after injection; PTX was not detected after 24 h or later of injection. The plasma concentration at 5 min ($C_{5\ min}$) and the AUC of NK105 were 11- to 20-fold and 50- to 86-fold higher for NK105 than for PTX, respectively. Furthermore, the half-life at the terminal phase ($t_{1/2z}$) was 4 to 6 times longer for NK105 than for PTX. The maximum concentration (C_{max}) and AUC of NK105 in Colon 26 tumors were approximately 3 times and 25 times higher for NK105 than for PTX, respectively. NK105 continued to accumulate in the tumors until 72 h after injection. The tumor PTX concentration was higher than 10 μg/g even at 72 h after the intravenous injection of NK105 50 and 100 mg/kg. By contraries, the tumor PTX concentrations at 72 h after the intravenous administration of free PTX 50 and 100 mg/kg were below detection limits and less than 0.1 μg/g, respectively.

2.3. In vivo antitumor activity

BALB/c mice bearing s.c. HT-29 colon cancer tumors showed decreased tumor growth rates after the administration of PTX and NK105. However, NK105 exhibited superior antitumor activity as compared with PTX ($P<0.001$). The antitumor activity of NK105 administered at a PTX-equivalent dose of 25 mg/kg was comparable to that obtained after the administration of free PTX 100 mg/kg. Tumor suppression by NK105 increased in a dose-dependent manner. Tumors disappeared after the first dosing to mice treated with NK105 at a PTX-equivalent dose of 100 mg/kg, and all mice remained tumor-free thereafter (Fig. 2). In addition, less weight loss was induced in mice which were given NK105 100 mg/kg than in those which were given the same dose of free PTX(data not shown).

2.4. Neurotoxicity of PTX and NK105

Treatment with PTX has resulted in cumulative sensory-dominant peripheral neurotoxicity in humans, characterized clinically by numbness and/or paraesthesia of the extremities. Pathologically, axonal swelling, vesicular degeneration, and demyelination were observed. We, therefore, examined the effects of free PTX and NK105 using both electrophysiological and morphological methods.

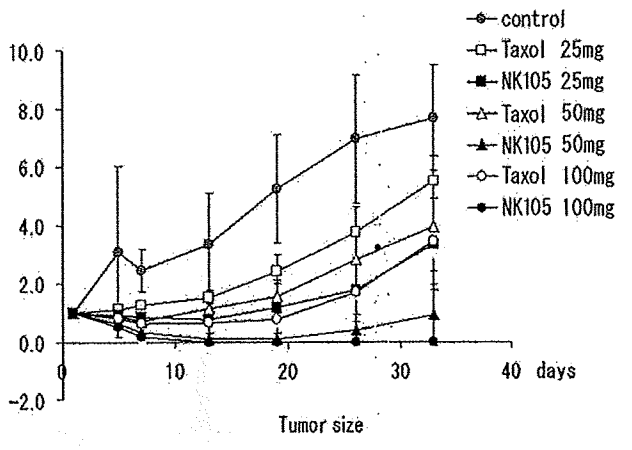

Fig. 2. Effects of PTX (open symbols) and NK105 (closed symbols). PTX and NK105 were injected intravenously once weekly for 3 weeks at PTX-equivalent doses of 25 mg/kg (□, ■), 50 mg/kg (△, ▲), and 100 mg/kg (○, ●), respectively. Saline was injected to animals in the control group (※) [12].

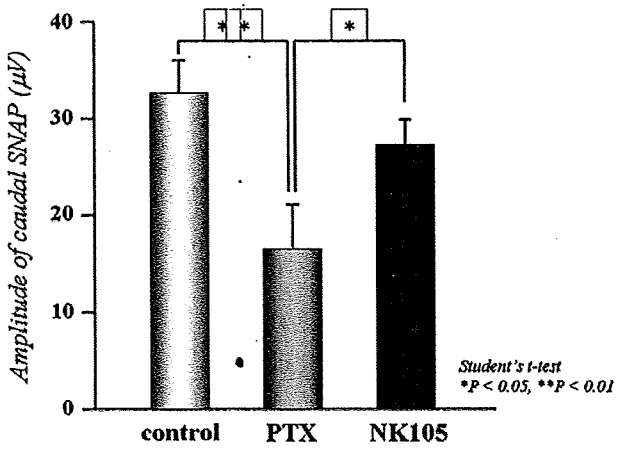

Fig. 3. Effects of PTX or NK105 on the amplitude of rat caudal sensory nerve action potentials as examined 5 days after weekly injections for 6 weeks. Rats (n=14) were injected with NK105 or PTX at a PTX-equivalent dose of 7.5 mg/kg. 5% glucose was also injected in the same manner to animals in the control group [12].

Prior to drug administration, there were no significant differences in the amplitude of caudal sensory nerve action potential (caudal SNAP) between two drug administration groups. On day 6 after the last dosing (at week 6), the amplitude of the caudal SNAP in the control group increased in association with rat maturation. The amplitude was significantly smaller in the PTX group than in the control group (P<0.01), while the amplitude was significantly larger in the NK105 group than in the PTX group (P<0.05) and was comparable between the NK105 group and the control group (Fig. 3). Histopathological examination of longitudinal paraffin-embedded sections of the sciatic nerve 5 days after the sixth weekly injection revealed degenerative changes. The NK105 administration group showed only a few degenerative myelinated fibers in contrast to the PTX administration group which indicated markedly more numerous degenerative myelinated fibers (data not shown).

2.5. NK105 has more potent radiosensitizing effect than free paclitaxel

Besides the antitumor activity of PTX, its ability to induce radiosensitization has been reported both in vitro [13–16] and *in vivo* [17–19] this effect has been attributed to its effect of stabilizing microtubules and inducing cell cycle arrest at the G2/M phase, the most radiosensitive phase of the cell cycle [20,21]. Since several clinical studies have demonstrated the efficacy of PTX-based chemotherapy combined with radiotherapy, the combined modality is considered to be a potentially important treatment option for lung and breast cancer [22,23].

The adverse effects of radiation, namely, lung toxicities in patients with breast or lung cancer treated by thoracic radiation,

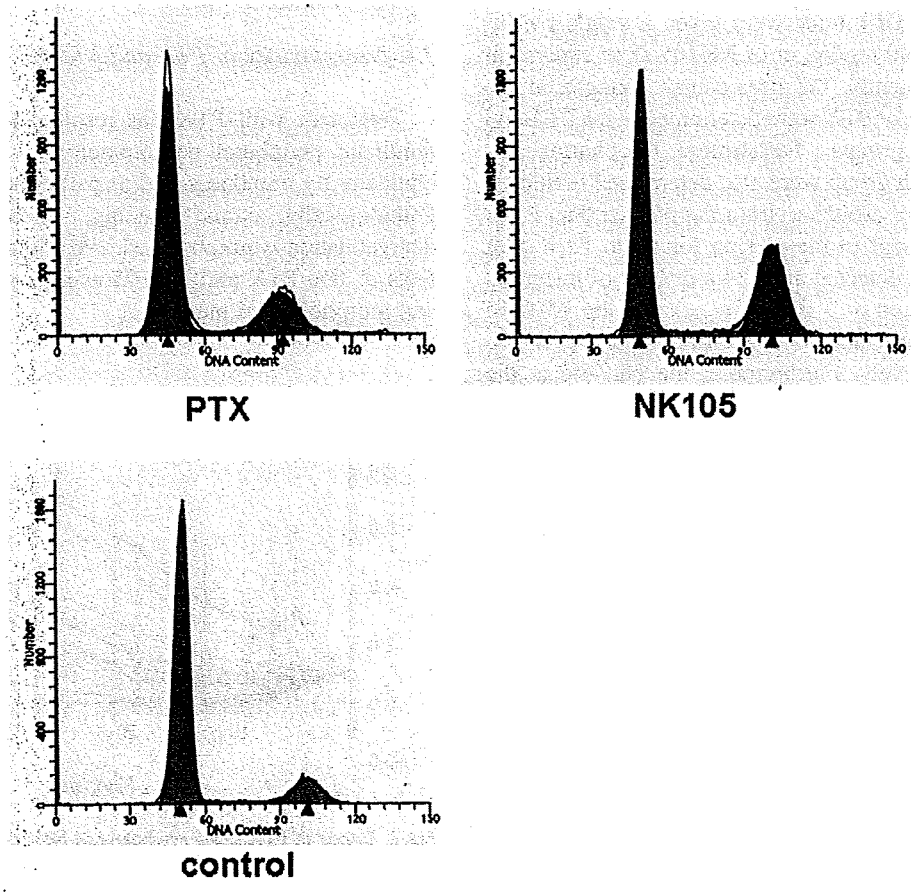

Fig. 4. Cell cycle analysis. Cell cycle analysis of LLC tumor cells 24 h after adding saline as a control, PTX or NK105 [28].

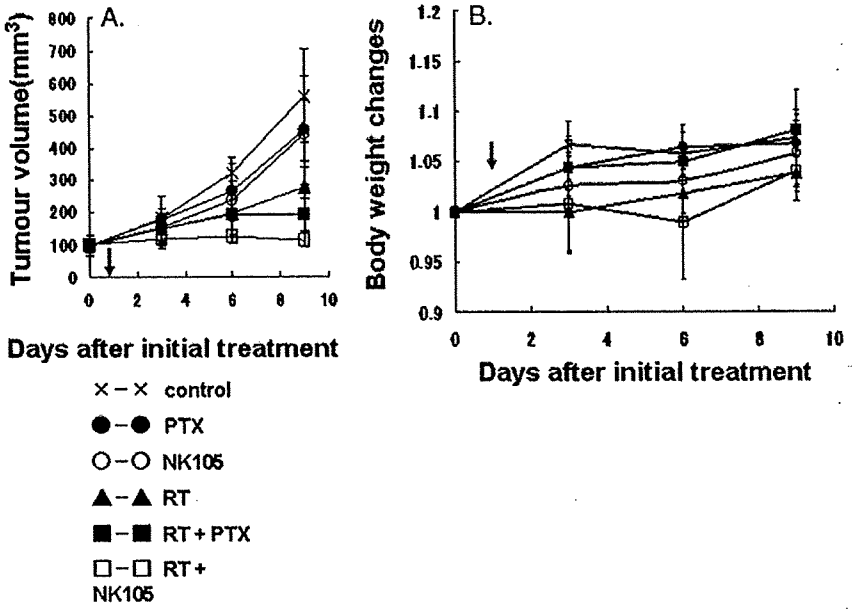

Fig. 5. Antitumor activity. Changes in the LLC tumor growth rates in the mice. (A) Mice receiving TXL-alone(●), NK105-alone(○), combined treatment with PTX and radiation(■), and combined treatment with NK105 and radiation(□) were administered a single i.v. injection of PTX or NK105 at the dose 45 mg/kg. Twenty-four hours after the drugs were administered, the mice in the radiation-alone (Δ)and the combined-treatment groups were irradiated. Mice in the control group (X) were given no treatment. (B) Changes in the relative body weight. Data were derived from the same mice as those used in the present study [28].

are of great concern, and may be dose-limiting or even have a negative impact on the quality of life of the patients, even though radiation is an efficient treatment option. Lung toxicities often result in lung fibrosis, necessitating change of the treatment method and causing much distress or even death of the patients [24,25]. Some clinical trials actually reported an increased incidence of pneumonitis following combined PTX therapy with radiation in patients with breast or lung cancer [26,27].

It is expected that the use of NK105 in place of PTX in combination with radiation may also yield superior results, because of the more potent antitumor activity of this drug as compared to that of free PTX. We evaluated the antitumor activity and severity of lung fibrosis induced by PTX and NK105 administered in combination with thoracic radiation, to examine whether combined NK105 chemotherapy with radiation would be an acceptable or useful treatment modality.

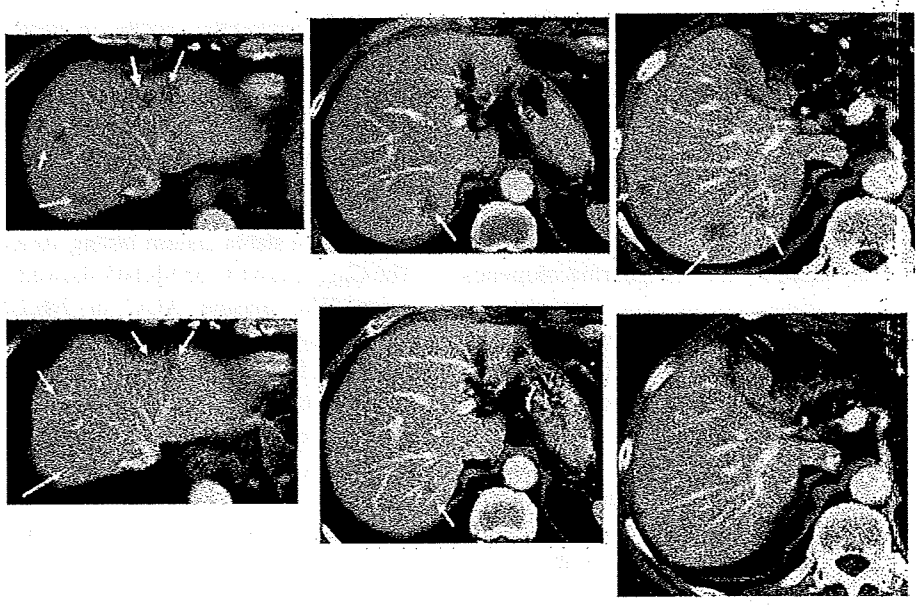

Fig. 6. Serial CT scans. A 60-year-old male with pancreatic cancer who was treated with NK105 at a dose level of 150 mg/m^2. Baseline scan (upper panels) showing multiple metastasis in the liver. Partial response, characterized by a more than 90% decrease in the size of the liver metastasis (lower panels) compared with the baseline scan. The antitumor response was maintained for nearly 1 year [29].

2.5.1. Cell cycle analysis

At 24 h after the administration of PTX or NK105 to the LLC-tumor-bearing mice, severe cell cycle arrest at the G2/M phase was observed in the tumor cells treated with the drugs as compared with that in the control (no drug treatment). There was a tendency towards the NK105-treated LLC tumor cells showing more severe arrest at the G2/M phase than the PTX-treated cells [28] (Fig. 4).

2.5.2. Antitumor activity

Decreased tumor growth rates of the LLC tumors were observed in the mice of the radiation alone, combined PTX with radiation, and combined NK105 with radiation groups [28]. No antitumor activity was observed following treatment with either PTX or NK105 alone, because LLC is primarily a PTX-resistant tumor. Combined NK105 therapy with radiation yielded superior antitumor activity as compared to both radiation alone ($P=0.0047$) and combined PTX therapy with radiation ($P=0.0277$) on the day 9 after the treatment initiation (Fig. 5A). No significant differences in body weight changes were noted among the groups tested (Fig. 5B).

2.5.3. Lung toxicities

Histopathological examination of the lung sections of all the mice receiving radiation showed inflammatory cell infiltration, appearance of intra-alveolar macrophages, and destruction of the alveolar architecture. Major portions of the alveolar septa in the lung sections prepared from the irradiated mice showed slight thickening, although no massive structural destruction was observed. On the other hand, the lung sections prepared from the control non-irradiated group showed no significant histopathological changes. Ashcroft's fibrosis scores in the groups of mice that received radiation ranged from 0.975 to 1.426, with no significant differences among the groups. The score in the control group was nearly zero. In the groups receiving radiation, the severity of lung fibrosis differed significantly among the mice within the same groups, as did the Ashcroft's scores, that is, the S.D. of the Ashcroft's scores in the mice receiving radiation was very high.

2.6. Clinical study

A phase I study was designed to determine maximum tolerated dose (MTD), dose-limiting toxicities (DLTs), the recommended dose (RD) for phase II and the pharmacokinetics of NK105 [29].

NK105 was administered by a 1-hour intravenous infusion every 3 weeks without anti-allergic premedication. The starting dose was 10 mg PTX equivalent/m^2, and dose escalated according to the accelerated titration method.

To date, 17 patients (pts) have been treated at the following doses: 10 mg/m^2 ($n=1$); 20 mg/m^2 ($n=1$); 40 mg/m^2 ($n=1$); 80 mg/m^2 ($n=1$); 110 mg/m^2 ($n=3$); 150 mg/m^2 ($n=5$); 180 mg/m^2 ($n=5$). Tumor types treated have included: pancreatic ($n=9$), bile duct ($n=5$), gastric ($n=2$), and colon ($n=1$). Neutropenia has been the predominant hematological toxicity and grade 3 or 4 neutropenia was observed in pts treated at 110, 150 and 180 mg/m^2. One patient at 180 mg/m^2 developed grade 3 fever. No other

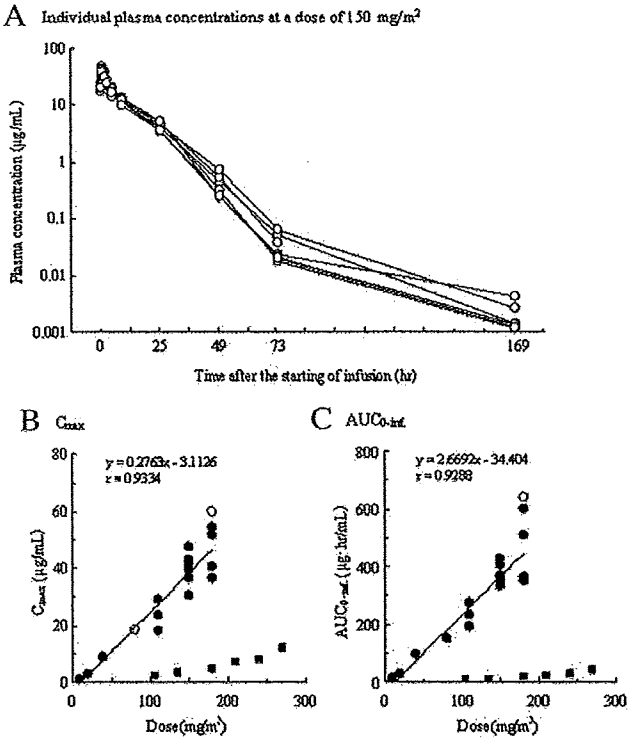

Fig. 7. (A) Individual plasma concentrations of PTX in 7 patients following 1 h intravenous infusion of NK105 at a dose of 150 mg/m^2. Relationships between dose and C_{max} (B), and between dose and AUC_{0-inf} (C) of PTX in patients following 1 h intravenous infusion of NK105. Regression analysis for dose vs. C_{max} was applied using all points except one patient at 80 mg/m^2 whose medication time became 11 min longer and one patient at 180 mg/m^2 who had medication discontinuation and steroid medication. (O) Regression analysis for dose vs. AUC_{0-inf} was applied using all points except one patient who had medication discontinuation and steroid medication. (O) Relationships between dose and C_{max}, and AUC_{0-inf} in patients following conventional PTX administration were plotted (closed square) [29].

grade 3 or 4 non-hematological toxicity including neuropathies was observed. DLTs were observed in pts with at the 180 mg/m^2 (grade 4 neutropenia lasting for more than 5 days), which was determined as MTD. Allergic reactions were not observed in any of the patients except one patient at level. A partial response was observed in one pancreatic cancer pt who received more than 12 courses of NK105 (Fig. 6). Despite of the long time usage, only grade 1 or 2 neuropathy was observed by modifying the dose or period of drug administration. Colon and gastric cancer pts experienced stable disease lasting 10 and 7 courses, respectively. The C_{max} and AUC of NK105 showed dose-dependent characteristics. The plasma AUC of NK105 at 180 mg/m^2 was approximately 30-fold higher than that of commonly-used paclitaxel formulation (Fig. 7).Accrual is ongoing at the 150 mg/m^2 dose level to determine RD. DLT was Grade 4 neutropenia. NK105 generates prolonged systemic exposure to PTX in plasma. Tri-weekly 1-hour infusion of NK105 was feasible and well tolerated, with antitumor activity in pancreatic cancer pt. A phase 2 study of NK105 against stomach cancer is now underway.

3. NC-6004, cisplatin-incorporating micellar nanoparticle

Cisplatin [*cis*-dichlorodiammineplatinum (II): CDDP] is a key drug in the chemotherapy for cancers, including lung,

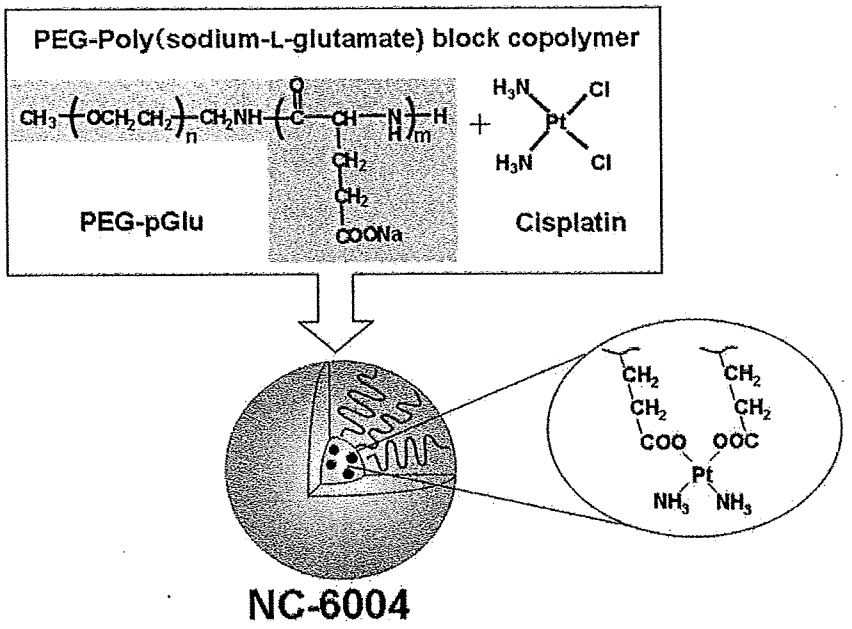

Fig. 8. Preparation and characterization of cisplatin-incorporating polymeric micelles (NC-6004). Chemical structures of cisplatin (CDDP) and polyethylene glycol poly(glutamic acid) block copolymers [PEG-P(Glu) block copolymers], and the micellar structures of CDDP-incorporating polymeric micelles (NC-6004) [39].

gastrointestinal, and genitourinary cancer [30,31]. However, we often find that it is necessary to discontinue treatment with CDDP due to its adverse reactions, e.g., nephrotoxicity and neurotoxicity, despite its persisting effects [32]. Platinum analogues, e.g., carboplatin and oxaliplatin [33], have been developed to date to overcome these CDDP-related disadvantages. Consequently, these analogues are becoming the standard drugs for ovarian cancer [34] and colon cancer [35]. However, those regimens including CDDP are considered to constitute the standard treatment for lung cancer, stomach cancer, testicular cancer [36], and urothelial cancer [37]. Therefore, the development of a drug delivery system (DDS) technology is anticipated, which would offer the better selective accumulation of CDDP into solid tumors while lessening its distribution into normal tissue.

3.1. Preparation and characterization of NC-6004

NC-6004 were prepared according to the slightly modified procedure reported by Nishiyama et al. [38,39] (Fig. 8). NC-6004 consists of polyethylene glycol (PEG), a hydrophilic chain which constitutes the outer shell of the micelles, and the co-ordinate complex of poly(glutamic acid) (P(Glu)) and CDDP, a polymer–metal complex-forming chain which constitutes the inner core of the micelles. The molecular weight of PEG-P(Glu) as a sodium salt was approximately 18,000 (PEG: 12,000; P (Glu): 6000). The CDDP-incorporated polymeric micelles were clearly discriminated from typical micelles from amphiphilic block copolymers. The driving force of the formation of the CDDP-incorporated micelles is the ligand substitution of platinum(II) atom from chloride to carboxylate in the side chain of P(Glu). The molar ratio of CDDP to the carboxyl groups in the copolymers was 0.71 [38]. A narrowly distributed size of polymeric micelles (30 nm) was confirmed by the dynamic light scattering (DLS) measurement. Also, the static light scattering (SLS) measurement revealed that the CDDP-loaded micelles showed no dissociation upon dilution and the CMC was less than 5×10^{-7}, suggesting remarkable stability compared with typical micelles from amphiphilic block copolymers [38]. It is assumed that the interpolymer cross-linking by Pt(II) atom might contribute to stabilization of the micellar structure.

Table 2
Pharmacokinetic parameter estimates for CDDP and NC-6004 in rats

Compound	Rat	T^{a}_{max} (h)	C^{a}_{max} (mg/mL)	$t_{1/2z}$ (h)	AUC_{0-t} (mg h/mL)	AUC_{0-inf} (mg h/mL)	CL_{tot} (mL/h/kg)	MRT_{0-inf} (h)	V_{ss} (L/kg)
CDDP	Mean	0.083	11.67	34.50	20.47	75.73	70.67	46.57	3.00
	S.D.		0.57	16.14	2.25	26.13	20.34	22.38	0.61
NC-6004	Mean	0.50	89.90	6.43	1325.90	1335.47	3.77	10.67	0.04
	S.D.		4.29	0.55	77.85	75.99	0.21	0.15	0.0023

See text for definitions of parameters.
The pharmacokinetic parameters were calculated after fitting to a non compartment model using WinNonlin program.
[a]For CDDP group, values of T_{max} and C_{max} represent 5 min and $C_{5\ min}$, respectively [39].

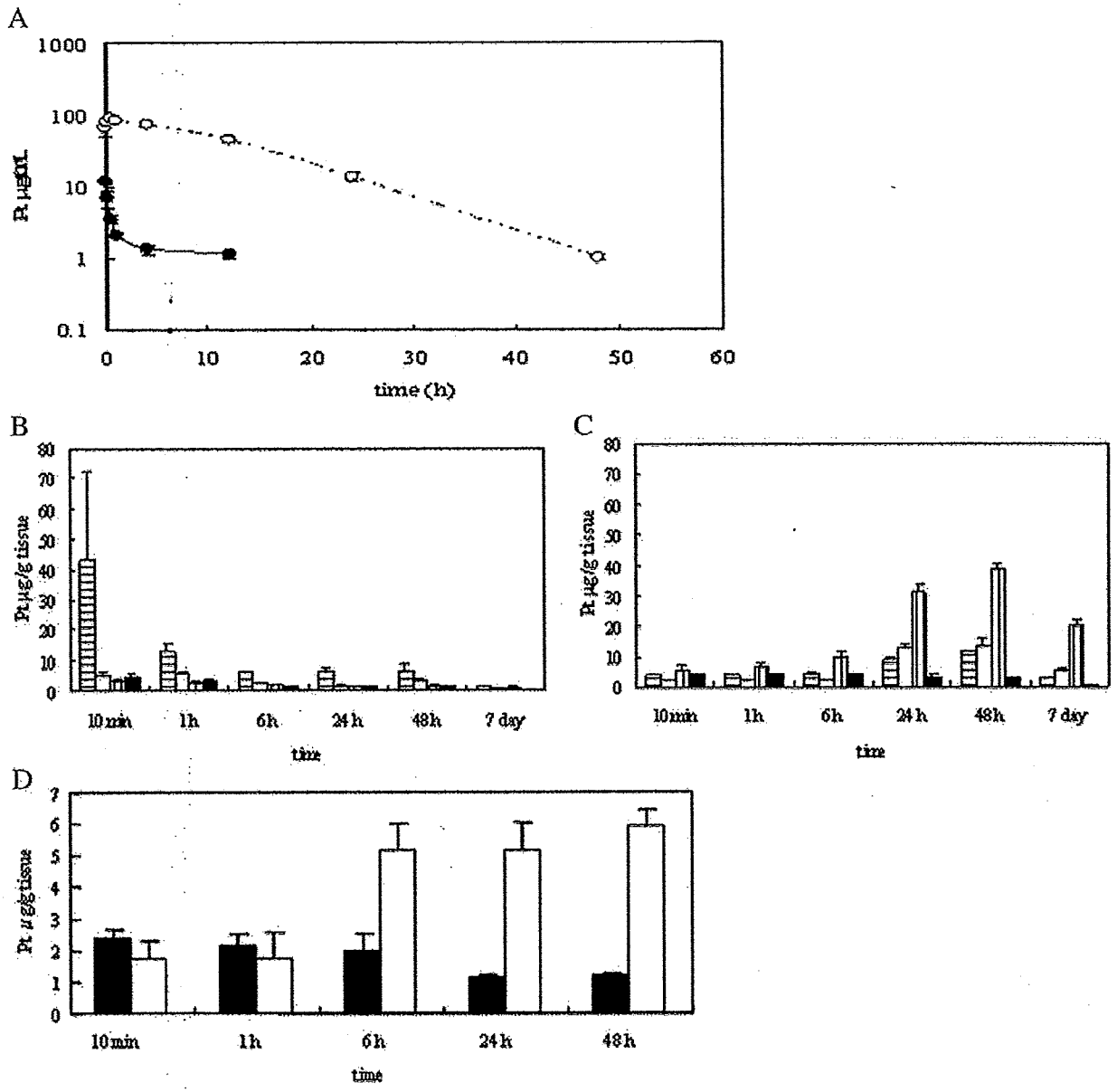

Fig. 9. Time profiles of platinum (Pt) concentration in the plasma and tissue distribution of Pt after a single i.v. injection of CDDP (5 mg/kg) or NC-6004 (an equivalent dose of 5 mg/kg CDDP). (A) Concentration-time profile of Pt in the plasma after a single i.v. injection of CDDP (●) and NC-6004 (○) in rats (n=3). Tissue distribution of platinum after a single i.v. injection of CDDP (B) and NC-6004 (C) in rats (n=3) (kidney (▥), liver (□), spleen (▤), and lung (■)). (D) Time profiles of platinum concentration in the MKN-45 solid tumor after a single i.v. injection of CDDP (■) and NC-6004 (□) in MKN-45 bearing BALB/c nude mice (n=3). Values are expressed as the mean±S.D [39].

The release rates of CDDP from NC-6004 were 19.6% and 47.8% at 24 and 96 h, respectively. In distilled water, furthermore, NC-6004 was stable without releasing cisplatin.

3.2. Pharmacokinetics and pharmacodynamics

FAAS could measure serum concentrations of platinum up to 48 h after i.v. injection of NC-6004 but could measure them only up to 4 h after i.v. injection of CDDP. NC-6004 showed a very long blood retention profile as compared with CDDP [39]. The AUC_{0-t} and C_{max} values were significantly higher in animals given NC-6004 than in animals given CDDP, namely, 65-fold and 8-fold, respectively ($P<0.001$ and $P<0.001$, respectively) (Table 2, Fig. 9A). Furthermore, the CL_{tot} and V_{ss} values were significantly lower in animals given NC-6004 than in animals given CDDP, i.e., one-nineteenth and one-seventy fifth, respectively ($P<0.01$ and $P<0.01$, respectively) (Table 2).

Regarding the concentration-time profile of platinum in various tissues after i.v. injection of CDDP or NC-6004, all organs measured exhibited the highest concentrations of platinum within 1 h after administration in all animals given CDDP (Fig. 9B). Furthermore, animals given NC-6004 exhibited the highest tissue concentrations of platinum in the liver and spleen at late time points (24 and 48 h after administration, respectively). However, the concentrations decreased on day 7 after administration (Fig. 9C). In addition, and in a similar manner to other drugs which are incorporated in polymeric carriers, NC-6004 demonstrated accumulation in organs of the

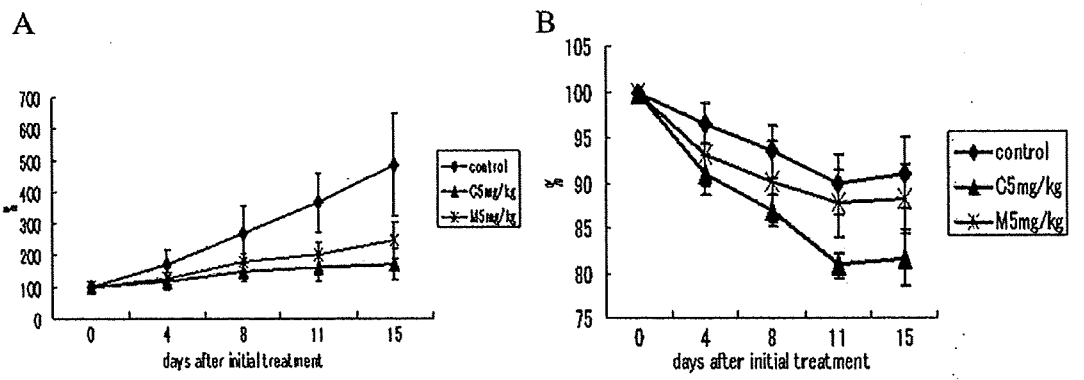

Fig. 10. Relative changes in MKN-45 tumor growth rates in nude mice. (A) CDDP(▲) and NC-6004(X) were injected intravenously every 3 days, 3 administrations in total, at CDDP-equivalent doses of 5 mg/kg. 5% glucose was injected in the control mice (◇). (B) Changes in relative body weight. Data were derived from the same mice as those used in the present study. Values are expressed as the mean±S.E [39].

reticuloendothelial system, e.g., liver and spleen. At 48 h after administration, tissue concentrations of platinum in the liver and spleen were 4.6- and 24.4-fold higher for NC-6004 than for CDDP. On the other hand, a marked increase in tissue platinum concentration was observed immediately after administration in the kidneys of animals given CDDP. Renal platinum concentration at 10 min and 1 h after administration were 11.6- and 3.1-fold lower, respectively, in animals given NC-6004 than in animals given CDDP. Furthermore, the maximum concentration (C_{max}) in the kidney was 3.8-fold lower at the time of NC-6004 administration than at the time of CDDP administration.

Regarding the tumor accumulation of platinum, tumor concentrations of platinum peaked at 10 min after administration of CDDP. On the other hand, tumor concentrations of platinum peaked at 48 h after administration of NC-6004 (Fig. 9D). The maximum concentration (C_{max}) in tumor was 2.5-fold higher for NC-6004 than for CDDP ($P<0.001$). Furthermore, the tumor AUC was 3.6-fold higher for NC-6004 than for CDDP (81.2 μg/mL h and 22.6 μg/mL h in animals given NC-6004 and CDDP, respectively).

3.3. In vivo antitumor activity

BALB/c nude mice implanted with a human gastric cancer cell line MKN-45 showed decreased tumor growth rates after i.v. injection of CDDP and NC-6004 (Fig. 10A). In the administration of CDDP, the CDDP 5 mg/kg administration group showed a significant decrease ($P<0.01$) in tumor growth rate as compared with the control group. However, the NC-6004 administration groups at the same dose levels as CDDP showed no significant difference in tumor growth rate. Regarding time-course changes in body weight change rate, the CDDP 5 mg/kg administration group showed a significant decrease ($P<0.001$) in body weight as compared with the control group. On the other hand, NC-6004 administration group did not show a decrease in body weight as compared with the control group (Fig. 10B).

3.4. Nephrotoxicity of CDDP and NC-6004

In the CDDP 10 mg/kg administration group, 4 of 12 rats died from toxicity within 7 days after drug administration. No deaths occurred in the NC-6004 10 mg/kg administration group. Regarding renal function, the BUN concentrations on day 7 after the administration of 5% glucose, CDDP 10 mg/kg, and NC-6004 10 mg/kg were 20.8±3.0, 65.3±44.4, and 20±4.5 mg/dL, respectively. The plasma concentrations of creatinine on day 7 after the administration of 5% glucose, CDDP 10 mg/kg, and NC-6004 10 mg/kg were 0.27±0.03, 0.68±0.23, and 0.28± 0.04 mg/dL, respectively. The CDDP 10 mg/kg administration group showed significantly higher plasma concentrations of BUN and creatinine as compared with the control group ($P<0.05$ and $P<0.001$, respectively), with the NC-6004 10 mg/kg administration group ($P<0.05$ and $P<0.001$, respectively) (Fig. 11A and B). Light microscopy indicated tubular dilation with flattening of the lining cells of the tubular epithelium in the kidney from all animals in the CDDP 10 mg/kg administration group. On the other hand, no histopathological change was observed in the kidneys from all animals in the NC-6004 10 mg/kg administration group.

3.5. Neurotoxicity of CDDP and NC-6004

Neurophysiological examination revealed that motor nerve conduction velocities (MNCVs) in animals given 5% glucose, CDDP, and NC-6004 were 44.2±3.5, 40.94±5.08, and 40.62± 0.63 m/s, respectively. No significant difference was found among the groups with respect to MNCV. Furthermore, sensory

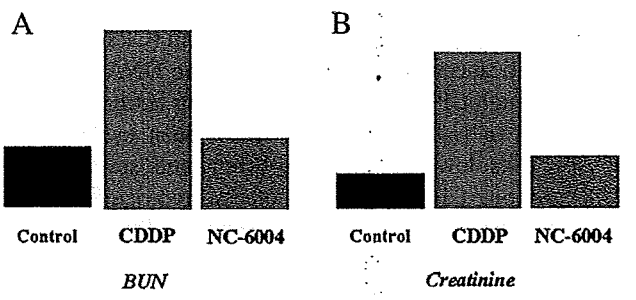

Fig. 11. Nephrotoxicity of CDDP and NC-6004. Plasma concentrations of blood urea nitrogen (BUN) and creatinine were measured after a single i.v. injection of 5% glucose ($n=8$), CDDP at a dose of 10 mg/kg ($n=12$), NC-6004 at a dose of 10 mg/kg ($n=13$) on a CDDP basis (modification of ref. [39]).